Available online at www.sciencedirect.com
ScienceDirect
Computational Materials Science 43 (2008) 229–234
COMPUTATIONAL MATERIALS SCIENCE
www.elsevier.com/locate/commatsci

Assessing failure in microelectronic compounds

K. Weinberg

Institute of Mechanics, Technical University of Berlin, Einsteinufer 5, 10587 Berlin, Germany

Available online 29 October 2007

Abstract

A strategy to estimate life expectation in copper vias is presented. To this end, two-scale finite-element simulations of thermal cycling are performed. The employed material model for the copper vias accounts for large elastic and plastic deformations and, additionally, for the growth of pores within the material.

The common practice to extrapolate the accumulated plastic strain computed within a few steps of thermal cycling by means of a Coffin–Manson equation is critical examined. It is pointed out that a relatively large number of steps is necessary to obtain meaningful results. Furthermore, it is demonstrated that an extrapolation of the computed porosity up to a critical value allows for analogous conclusions.

1. Introduction

Plated-through vias are little tubes which form conductive paths between the different layers of microelectronic circuit boards. Failure of these connectors due to thermo-mechanical stresses is a well known cause of failure of the whole circuit board. Therefore, the life expectation of plated-through vias is of great interest for the microelectronic industry.

Vias are commonly made of (electrolytically deposited) copper whereas the surrounding material is typical a non-isotropic resin, e.g., the glass fibre reinforced resin flame-retardant 4 material substrate (FR4). In order to ensure the required life expectation of circuit units standardized thermal cycle tests are performed. Due to the different thermal expansion coefficients of the copper and the anisotropic board the copper vias are highly stressed and strained. This leads to an accumulation of permanent irreversible strains associated with cracks and pores which eventually results in the electro-mechanical destruction of the connector. The issue of filling the plated-through vias with solder or solder stop mask (resin) and, if possible, to increase its life expectation as opposed to leaving it unfilled has been open to considerable debate, see, e.g. [2].

In this paper, we numerically study such copper vias subjected to thermal cycling between −40 °C and +150 °C (automotive standard), see Fig. 1. After introducing the general strategy and the employed material model we estimate the damage for plated-through vias with and without filling located at different positions in a multi-layer printed-circuit board (PC board) onto which a flip chip component has been mounted (FCOB = flip chip on board) and we suggest a technique for improved life time estimation.

2. Two-scale finite-element modelling

Compared to the PC board and the microelectronic components mounted thereon the plated-through vias are much smaller. If modelled directly this would lead to a finite-element mesh with an unnecessarily high amount of degrees of freedom. For that reason we make use of a sub-modelling technique. The global model consists of (one quarter of) the FCOB unit and the PC board, delicate substructures, such as the vias, are not included. The board is made of FR4, a resin with material data shown in Table 1. Symmetry conditions apply along the *diagonal* surfaces. The front surface

E-mail address: kerstin.weinberg@tu-berlin.de

0927-0256/$ - see front matter © 2007 Elsevier B.V. All rights reserved.
doi:10.1016/j.commatsci.2007.07.049

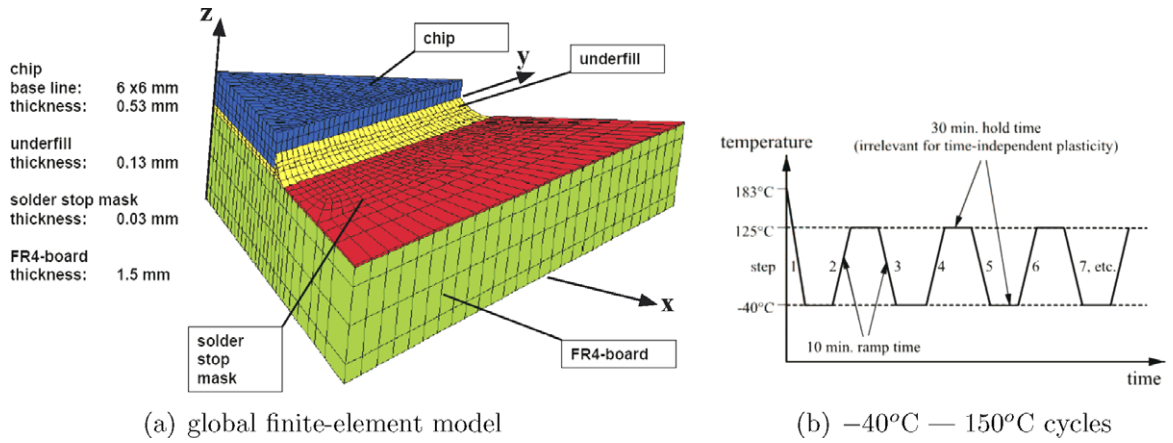

Fig. 1. Finite-element model of a FCOB circuit unit loaded by temperature cycles: (a) global finite-element model, (b) – 40 °C to 150 °C cycles.

Table 1
Material parameter of temperature dependent FR4 material

T (K)	E_x, E_y	E_z (MPa)	ν_{xy}	ν_{xz}, ν_{yz}	G_{xz}, G_{yz}	G_{xy} (MPa)	α_x, α_y	α_z (ppm/K)
223	14,218	7109	0.15	0.4	2539	6182	1.7×10^{-5}	6×10^{-5}
373	12,166	6083	0.15	0.4	2172	5290	1.7×10^{-5}	6×10^{-5}
461	3038	1519	0.15	0.4	542	1320	1.7×10^{-5}	6×10^{-5}

was forced not to tilt but rather to move in a straight manner in order to mimic the embodiment of the package within the whole assembly. Temperature cycles are imposed; the initial value of 183 °C refers to the melting temperature of eutectic SnPb solder which was assumed to be the stress free state of reference.

In a second step finite-element submodels of the vias are created. The dimensions are as follows: width of the basal plane 1.0 mm, wall thickness of the copper cylinder 0.022 mm, inner diameter 0.256 mm, outer diameter 0.65 mm, height of the submodel 1.5 mm. The copper via is surrounded by the orthotropic FR4 resin; at the upper and lower surface it is covered by a thin layer of solder stop mask, see Fig. 2. Both, temperature steps and the deformations that result from the finite-element analysis (FEA) of the global model are now extrapolated and imposed onto the periphery of the local models.

During the manufacturing of plated-through vias the copper is electrolytically deposited, hence, the mechanical properties may differ significantly from those of bulk copper. Here we make use of material data provided by IBM electronics and published in [3], see Table 2. Hardening of the yield stress is described with a power-law function,

$$\sigma_y = \sigma_{y_0}(T)\left(1+\frac{\varepsilon^p}{\varepsilon_0^p(T)}\right)^{1/n}, \tag{1}$$

where the initial yield stress $\sigma_{y_0}(T)$ and the reference plastic strain $\varepsilon_0^p(T)$ account for a temperature dependence of plasticity. The hardening exponent is assumed constant with $n = 25$.

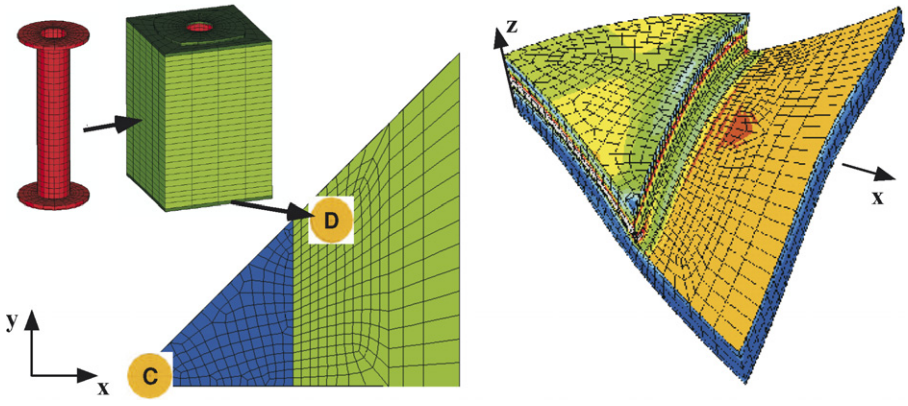

Fig. 2. Submodel of unfilled copper vias, positions within the global structure and, to the left, von Mises stress distribution in the deformed circuit unit (stress maxima in red). (For interpretation of the references to colour in this figure legend, the reader is referred to the web version of this article.)

Table 2
Material parameter of solder stop mask (top) and copper (bottom)

T (K)	E (MPa)	ν		
Solder stop mask				
218	6000	0.34		
373	2500	0.42		
423	1000	0.45		
T (K)	E (MPa)	ν	σ_{y_0} (MPa)	ε_0^p
Copper				
208	45,086	0.34	156	0.00346
473	39,285	0.34	121	0.00308
573	31,028	0.34	87.5	0.00282

3. Material model of electrolytically deposited copper

Engineering metals contain a certain amount of cavities, such as vacancies in the crystal lattice or, simply, pores arising during manufacturing. By electrolytical deposition of copper the initial porosity, i.e., the volume of pores per unit volume, is expected to be relatively high and we assume $f_{V0} = 10^{-3}$. The growth and finally coalescence of such pores in highly strained material is the basic failure mechanism in ductile fracture, cf., e.g. [4].

To account for both damaging mechanisms, i.e., shear induced plastic straining and growing porosity in the copper material, we employ a material model that combines classical von Mises plasticity with volumetric plasticity. The model accounts for the full kinematics of large deformations and assumes a multiplicative decomposition of the deformation gradient into elastic and plastic parts, $\boldsymbol{F}^e$ and $\boldsymbol{F}^p$, respectively,

$$\boldsymbol{F} = \boldsymbol{F}^e\boldsymbol{F}^p \Rightarrow \boldsymbol{F}^e = \boldsymbol{F}\boldsymbol{F}^{p^{-1}}. \tag{2}$$

By use of logarithmic strains the subsequent equations can in part be written in the more familiar terms of strain tensor $\boldsymbol{\epsilon}$ with elastic and plastic components, $\boldsymbol{\epsilon}^e$ and $\boldsymbol{\epsilon}^p$,

$$\boldsymbol{\epsilon} = \frac{1}{2}\ln(\boldsymbol{F}^\top\boldsymbol{F}), \quad \boldsymbol{\epsilon}^e = \frac{1}{2}\ln(\boldsymbol{F}^{e\top}\boldsymbol{F}^e) \quad \text{and} \quad \boldsymbol{\epsilon} = \boldsymbol{\epsilon}^e + \boldsymbol{\epsilon}^p. \tag{3}$$

We postulate the existence of a free-energy density of the material of the form

$$A(\boldsymbol{F}, \boldsymbol{F}^p, \varepsilon^p, \vartheta^p, T) = W^e(\boldsymbol{F}^e, T) + W^p(\varepsilon^p, \vartheta^p, T), \tag{4}$$

where W^e and W^p denote the elastic and stored plastic energy densities per unit undeformed volume, respectively. Moreover, the internal variable ε^p describes the accumulated plastic straining, ϑ^p measures the accumulated volumetric plastic expansion and T is the absolute temperature. Time-dependence of the material, such as rate-sensitivity or creep is of minor influence here and thus neglected (see Fig. 3).

With the bulk modulus $\kappa = E/(3(1-2\nu))$, the thermal expansion coefficient α, the mass density ϱ_0, the specific heat per unit mass c_v and the relations (3) the elastic energy density reads

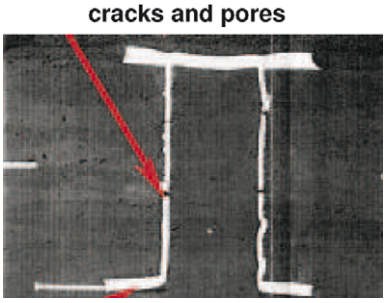

Fig. 3. Via, experimentally studied in [1].

$$W^e = \frac{1}{2}\kappa(\operatorname{tr}\boldsymbol{\epsilon}^e - 3\alpha(T-T_0))^2 + \varrho_0 c_v T\left(1 - \ln\frac{T}{T_0}\right) + \frac{2}{3}\frac{2E}{1+\nu}|\operatorname{dev}\boldsymbol{\epsilon}^e|^2. \tag{5}$$

The plastic energy density is constructed to prescribe hardening of the yield stress according to Eq. (1), the volumetric component $W^{p,vol}$ will be specified below.

$$W^p = W^{p,dev}(\varepsilon^p, T) + W^{p,vol}(\vartheta^p, T) = \frac{n\sigma_y(T)\varepsilon_0^p(T)}{n+1}\left(1 + \frac{\varepsilon^p}{\varepsilon_0^p}\right)^{\frac{n+1}{n}} + W^{p,vol}(\vartheta^p, T). \tag{6}$$

The plastic deformation rate is assumed to obey the flow rule

$$\dot{\boldsymbol{F}}^p\boldsymbol{F}^{p-1} = \dot{\varepsilon}^p\boldsymbol{M} + \dot{\vartheta}^p\boldsymbol{N}, \quad \text{with} \quad \dot{\varepsilon}^p \geqslant 0, \ \dot{\vartheta}^p \geqslant 0, \tag{7}$$

where the tensors $\boldsymbol{M}$ and $\boldsymbol{N}$ set the direction of the deviatoric and volumetric plastic deformation rates, respectively. They are assumed to satisfy

$$\operatorname{tr}\boldsymbol{M} = 0, \quad \boldsymbol{M}\cdot\boldsymbol{M} = \frac{3}{2}, \quad \boldsymbol{N} = \pm\frac{1}{3}\boldsymbol{I}, \tag{8}$$

with the plus sign in $\boldsymbol{N}$ corresponding to pore expansion, and the minus sign to pore shrinkage. The tensors $\boldsymbol{M}$ and $\boldsymbol{N}$ are otherwise unknown and must be determined as part of the solution. The constraints (8) may be regarded as defining the assumed kinematics of plastic deformation.

The continuum measure of volumetric deformation will now directly be related to the porosity of the material. Through this connection we deduce the stored plastic energy function from the analysis of an ensemble of pores. For simplicity we assume a dilute distribution of spherical pores each surrounded by a spherical shell of material. The pores may grow but retain their shape whereas the matrix material follows von Mises plasticity, i.e., it is incompressible during plastic straining. This is, of course, a very simplified approach, however, it enables us to deduce the properties of the porous ensemble from a single spherical shell. For details of the model and a comparison with other approaches we refer to [5].

Consider a representative material of undeformed volume, V_0, and deformed volume, V, which are related by the local Jacobian of the deformation, $V = JV_0$. It follows that

$$J \equiv \det \boldsymbol{F} = \det(\boldsymbol{F}^{\mathrm{e}}\boldsymbol{F}^{\mathrm{p}}) = J^{\mathrm{e}}J^{\mathrm{p}} \Rightarrow J^{\mathrm{p}} = \frac{V}{J^{\mathrm{e}}V_0}. \tag{9}$$

We now define the current mean pore radius $\bar{a} \equiv \bar{a}(t)$. Then, by neglecting the elastic volume change of the voids, we can write for the plastic Jacobian J^{p} of a body with N spherical pores per volume (index 0 refers to the initial state) and its porosity

$$J^{\mathrm{p}} = 1 - f_{\mathrm{V0}} + N\frac{4\pi\bar{a}^3}{3} \Longleftrightarrow f_{\mathrm{V}} = \frac{f_{\mathrm{V0}} + J^{\mathrm{p}} - 1}{J^{\mathrm{p}}}. \tag{10}$$

These functions relate the mean pore radius $\bar{a}$ and J^{p} one-to-one.

From spherical symmetry and the plastic incompressibility constraint (for the matrix material) we derive the strain rate of a material sphere with radius r surrounding a pore and undergoing with the solid plastic deformations

$$\frac{\mathrm{d}}{\mathrm{d}t}\frac{4\pi(r^3 - \bar{a}^3)}{3} = 0 \Rightarrow \dot{\varepsilon}^{\mathrm{p}}(r,t) = \left|\frac{\partial \dot{r}}{\partial r}\right| = \frac{2\bar{a}^2(t)}{r^3(t)}|\dot{\bar{a}}(t)|. \tag{11}$$

Now we suppose that the mean pore radius $\bar{a}(t)$ grows monotonically from $\bar{a}_0$ to $\bar{a}_1$, then decreases monotonically from $\bar{a}_1$ to $\bar{a}_2$, and so on. Integration of (11) with respect to time gives the plastic strain

$$\begin{aligned}\varepsilon^{\mathrm{p}}(r_0) = {} & \frac{2}{3}\ln\left(\frac{\bar{a}_1^3 + r_0^3 - \bar{a}_0^3}{r_0^3}\right) + \frac{2}{3}\ln\left(\frac{\bar{a}_1^3 + r_0^3 - \bar{a}_0^3}{\bar{\bar{a}}_2^3 + r_0^3 - a_0^3}\right) \\ & + \frac{2}{3}\ln\left(\frac{\bar{a}_3^3 + r_0^3 - \bar{a}_0^3}{\bar{a}_2^3 + r_0^3 - \bar{a}_0^3}\right) + \cdots.\end{aligned} \tag{12}$$

For purely volumetric deformation the deformation gradient is of the spherical form $\boldsymbol{F} = J^{1/3}\boldsymbol{I}$ and flow rule (7) reduces to $\ln(J^{\mathrm{p}})\boldsymbol{I} = \vartheta^{\mathrm{p}}\boldsymbol{N}$. Evaluation yields

$$\frac{\mathrm{d}}{\mathrm{d}t}\ln(J^{\mathrm{p}}) = \operatorname{tr}\boldsymbol{N}\dot{\vartheta}^{\mathrm{p}} = \pm\dot{\vartheta}^{\mathrm{p}} \Rightarrow \dot{\vartheta}^{\mathrm{p}} = \left|\frac{\mathrm{d}}{\mathrm{d}t}\ln J^{\mathrm{p}}\right| \quad \text{and}$$

$$\vartheta^{\mathrm{p}}(t) = \vartheta^{\mathrm{p}}(0) + \int_0^t \dot{\vartheta}^{\mathrm{p}}(\xi)\mathrm{d}\xi. \tag{13}$$

Note that the variable ϑ^{p} is a measure of the *accumulated* volumetric plastic deformation. For monotonic expansion ϑ^{p} and $\ln(J^{\mathrm{p}})$ coincide up to a constant. For an arbitrary loading history the value of $\vartheta^{\mathrm{p}}(t)$ rises even when the pores shrink and the information about actual pore size is in general solely in $J^{\mathrm{p}}(t)$ via relation (10). The physical constraint $J^{\mathrm{p}} \geqslant 1$ applies, i.e., the pores are not allowed to be smaller than the initial pore size.

The stored energy for a spherical pore in a power-law hardening material equals the plastic work of deformation attendant to its expansion or contraction. Applied to the spherical shell model this leads to the volumetric component of plastic work

$$W^{\mathrm{p,vol}}(\bar{a},T) = N\int_{a_0}^{b_0}\frac{n\sigma_0(T)\varepsilon_0^{\mathrm{p}}}{n+1}\left(1 + \frac{\varepsilon^{\mathrm{p}}(r_0)}{\varepsilon_0^{\mathrm{p}}(T)}\right)^{\frac{n+1}{n}} 4\pi r_0^2\,\mathrm{d}r. \tag{14}$$

Following the classical thermo-mechanical approach the stresses result from the derivative of the energy densities with respect to the conjugate deformation variable (cf. [6,5] for the variational framework and evaluated expressions).

4. Structural response and life expectation

It is common practise to simulate only a few steps of the temperature cycling and extrapolate the results until fatigue failure is anticipated, cf. [1,2]. Following this approach we apply a temperature history of five steps to analyze vias filled with solder stop mask and empty vias located at several positions of the board.

The vias are – to a different extent – strained mostly in the middle of the copper cylinder. The initial cooling causes a considerable plastic strain but no plastic dilatation. The copper tubes seem to bend under pressure due to the different thermal expansion coefficients. Rising temperature causes tension and pores to grow but hardly plastic strain. The process repeats with smaller amplitude. The vias that are strained mostly are located at the middle of the unit (position C) and along the diagonal (position D), see Figs. 1 and 4.

The fatigue resistance of a structure is commonly estimated by using a Coffin–Manson relation,

$$\frac{\Delta\varepsilon^p}{2} = \varepsilon_{\mathrm{f}}(2N_{\mathrm{f}})^c, \tag{15}$$

where $(2N_{\mathrm{f}})$ is the number of strain reversals (cycles), ε_{f} is the ductility (here 20%) and the exponent c is empirically set -0.6 for most metals. We apply this relation to the computed strain increments. However, the first step is skipped because the initial cooling gives no information about a typical life cycle. The life expectations computed with the maximum straining per step (averaged over the integration points of the element) are summarized in Table 3. The calculated numbers of steps are low with respect to the required life expectation of at least $N_{\mathrm{f}} = 8000$. Moreover this approach does not account for the fact that the absolute value of ε^{p} is higher for the vias filled with solder stop mask.

To answer the question of how reliable this approach is we now compare with a temperature history of 21 steps and analyze the plastic strain as well as the expected pore growth. The distribution of plasticity is displayed in Fig. 5 and nicely reflects the loading of the vias. In position D bending dominates and the accumulated plastic strain and, in particular, the plastic volumetric expansion show a localization on the sides of the via. In position C (direct underneath the chip) the via is mainly stretched along its axis and the distribution of plasticity in circumferential direction is basically homogeneous. The highest plastic strain is accumulated in the upper half of the copper tube, whereas the pores and voids grow increasingly towards the lower half. If we superimpose both defects there seems to be a higher probability of failure within the middle parts of the vias. Clearly, here is some need to substantiate such an effect experimentally.

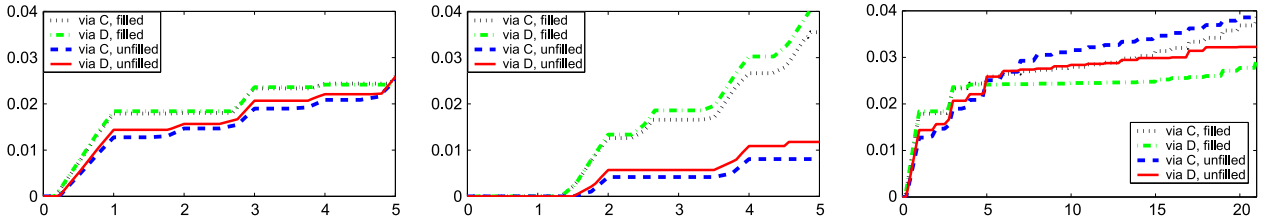

(a) plastic strain ε^p, 5 steps (b) vol. expansion ϑ^p, 5 steps (c) plastic strain ε^p, 21 steps

Fig. 4. Temporal development of the maxima of plasticity over temperature steps: (a) plastic strain ε^{p}, five steps; (b) vol. expansion ϑ^{p}, five steps and (c) plastic strain ε^{p}, 21 steps.

Table 3
Life expectation of vias estimated with different approaches

Via	Five temperature steps	Twenty-one temperature steps		
	$N_{\mathrm{f}}(\varepsilon^{\mathrm{p}})$	$N_{\mathrm{f}}(\varepsilon^{\mathrm{p}})$	$N_{\mathrm{f}}(f_{\mathrm{V}})$, $e=1$	$N_{\mathrm{f}}(f_{\mathrm{V}})$, $e=0.9$
C, no filling	1684	4529	1361	3035
C, filling	525	4942	2036	4746
D, no filling	591	15,818	6592	17,512
D, filling	1867	21,490	15,372	44,866

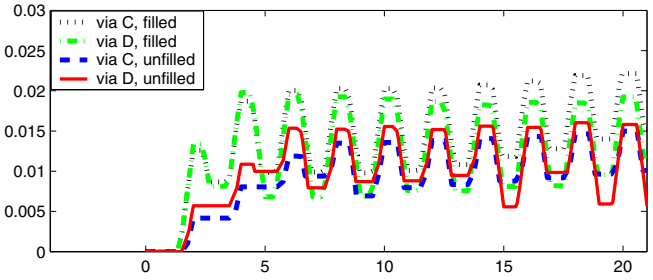

Fig. 6. Development of pore growth measured with $\ln(J_{\mathrm{p}})$ within 21 temperature steps.

For all vias studied the first steps initiates a considerable amount of plastic straining with amplitudes higher in the filled than in the unfilled vias. Within the next temperature steps the strain increments $\Delta\varepsilon^{\mathrm{p}}$ decay and show a certain saturation. Clearly, $\Delta\varepsilon^{\mathrm{p}}$ computed from a FEA of five temperature steps is not representative for the rest of the life cycle (see Fig. 4 and Table 3). The numbers of expected life cycles are by an order of magnitude larger. Furthermore, filling a via should be beneficial for its life expectation.

To account for growth and shrinkage of pores let us now monitor the plastic volume change, J_{p}, during 21 temperature steps, Fig. 6. In all vias the first heating causes a significant growth in porosity. Then, similar to the plastic straining, a certain saturation is reached after approximately six steps. Thenceforward pores in the copper material open and close with every temperature cycle. The resulting porosity shows a slight increase in every cycle.

An empirical equation to estimate the life time of a material from its porosity is not known. Here we suggest an estimate from the mean increase of porosity during a temperature cycle, Δf_{V}, computed from the plastic volume change via Eq. (10). With f_{V0} and $f_{\mathrm{V_f}}$ being the initial and the failure porosity (here 0.3) that gives

$$\Delta f_{\mathrm{V}} = (f_{\mathrm{V_f}} - f_{\mathrm{V0}})/(N_{\mathrm{f}})^{e} \Rightarrow N_{\mathrm{f}} = ((f_{\mathrm{V}_f} - f_{\mathrm{V0}})/\Delta f_{\mathrm{V}})^{1/e}. \tag{16}$$

Extrapolating Δf_{V} in a linear manner, i.e., $e=1$, shows the same tendency but lower values like the extrapolated plastic strain. Allowing for a slight decay of the curve, $e=0.9$, gives results that nicely correspond to the Coffin–Manson estimate. Both criteria yield qualitatively equal results and show the unfilled via at position C being the most likely to fail. Fillings support the vias, in particular, in a tension–compression dominated state.

The presented analysis of plated trough vias shows that both mechanisms, plastic straining and the growth of pores within the copper via have an essential influence on the life time expectation of the vias and, in consequence, the whole circuit unit.

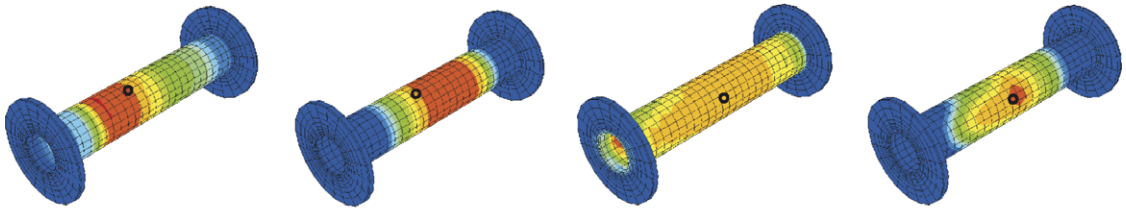

(a) C: plastic strain ε^p (b) C: expansion ϑ^p (c) D: plastic strain ε^p (d) D: expansion ϑ^p

Fig. 5. Distribution of accumulated plasticity in unfilled vias at position C and D (maxima: red, minima: blue), the location of the maxima is marked. (For interpretation of the references to colour in this figure legend, the reader is referred to the web version of this article.)

References

[1] H.J. Albrecht, J. Jendry, W.H. Müller, C. Wieand, in: Proc. of SMTA 201–208, Hawaii, 2003.
[2] D.B. Barker, A. Dasgupta, in: J.H. Lau (Ed.), Thermal Stress and Strain in Microelectronic Packaging, New York, 1993.
[3] J.C. DiTomasso. Stress analysis of vias within general electric's multichip modules, 2000, http://www.ecs.umass.edu/mie/labs/mda/fea/ditomaso/Main.htm.
[4] V. Tvergaard, Advances in Applied Mechanics 27 (1990) 83–151.
[5] K. Weinberg, Material models of microstructured solids – theory, numeric and applications. Habilitation Thesis, TU Berlin, 2007.
[6] K. Weinberg, A. Mota, M. Ortiz, Computational Mechanics 37 (2) (2006) 142–152.